EVALUATION OF SQUIRREL-CAGE FANS FOR HVAC APPLICATIONS IN PUBLIC TRANSPORT: KEY PARAMETERS AND DESIGN GUIDELINES

Sandra VELARDE-SUÁREZ, F. Israel GUERRAS COLÓN, Rafael BALLESTEROS-TAJADURA, José GONZÁLEZ, Katia M. ARGÜELLES DÍAZ, Jesús M. FERNÁNDEZ ORO, Carlos SANTOLARIA MORROS

UNIVERSIDAD DE OVIEDO, Departamento de Energía, Edificio Departamental Este, Campus Universitario, 33203 Gijón, España

SUMMARY

Small centrifugal and axial fans are used in automobile applications, as it is the case for HVAC systems for public transport. In particular, a specific type of centrifugal fans named "squirrel-cage" is broadly used in these systems. In this work, a morphological and functional characterization of up to 15 ventilation equipment used in commercial HVAC systems for public transport is carried out. The analysis of the obtained results is applied to select the best alternative among those analysed, focusing on energy efficiency and minimum noise generation criteria. In this way, the most important design criteria are established in order to get more efficient and less noisy ventilation systems.

INTRODUCTION

The design of fans for HVAC applications in public transport is nowadays based on benchmarking practices between the leading manufacturers worldwide. Focused on the economical aspects rather than innovating on new concepts, the current designs are typically based on tiny modifications over well-mature, finished products, leading to an oversupply of similar small fan units in the global market. At this point, a reformulation of the basic parameters required for new designs and the proposal of practical guidelines for manufacturers become really necessary to improve the overall R&D cycle in the near future.

Small centrifugal and axial fans are used in automobile applications. In particular, a specific type of centrifugal fans named "squirrel-cage" is broadly used in these systems. Their main geometrical characteristics are a large number of short chord forward-curved blades, and a rotor exit-to-inlet area ratio unusually large (Kind and Tobin [1]). Due to its size and relative high specific speed, these fans are used in applications with requirements of compact size, high flow rate and low cost. Typically, these fans are used to work at high rotation speed (over 4000 rpm) and variable operation conditions, even at extreme off-design points. Flow instabilities, low efficiency and high levels of noise and vibrations appear in these machines due to these working characteristics and to the need

for low fabrication costs. A basic feature of their impellers is the deficient flow guiding, as a result of the short radial length of the blades and their strong curvature. This effect is counterbalanced by a greater number of blades. Such an arrangement can cause the flow to stall, even at design conditions. Cau et al. [2] show in their work that the poor design of the flow channel in these fans causes a severely distorted primary flow, with early flow separation on the suction side at both low and design flow rates. They ascribed the inefficiencies of these machines to the sharp axial to radial bend, the large inlet gap between inlet nozzle and impeller shroud and poor matching between impeller outlet and volute tongue.

This paper completes a thorough review of commercial squirrel-cage fans from leading manufacturers in terms of geometry and both aerodynamic and noise performance. Based on twin-impeller, forward-curved centrifugal configuration, a benchmarking with 15 different commercial units has been carried out in this study, ranging most significant geometrical and operational parameters for comparison. Experimental data concerning best-efficiency points, overall efficiency range, noise generation and performance have been obtained in a test facility built according to standardized industrial normative.

Basic geometrical characteristics and best-efficiency points have been correlated in order to match performance variables with design parameters. Special attention has been paid on the optimal values required to minimize flow disturbances, to reduce the impeller-volute interaction and control the noise generation. A detailed classification of the different factors affecting the overall trend for the performance curves is also provided for every family of centrifugal fans tested, trying to identify the impact of every single parameter on the global behaviour of the fans.

NOMENCLATURE

b = impeller width (m)
BPF = blade passing frequency
D = diameter (m)
d_s = specific diameter $\left(\frac{D_2 \cdot \left(\frac{P_T}{\rho}\right)^{1/4}}{Q^{1/2}}\right)$
Lp = sound pressure level (dB)
f = frequency (Hz)
n_s = specific speed $\left(\frac{\omega \cdot Q^{1/2}}{\left(\frac{P_T}{\rho}\right)^{3/4}}\right)$
p = static pressure (Pa)
p_0 = reference acoustic pressure (20 μPa)
P = pressure (Pa)
Q = flow rate (m^3/h)
S = solidity $\left(\frac{\frac{D_2 - D_1}{2}}{\pi \cdot \left(\frac{D_1}{z}\right)}\right)$
W = power consumption (W)
z = number of blades
Δr = distance between volute tongue and impeller periphery (m)

Greek Letters

ρ = density (kg/m^3)
ω = angular velocity (rpm)
ψ = total pressure coefficient $\left(\frac{P_T}{\rho\omega^2 D_2^2}\right)$
η = efficiency
Φ = flow rate coefficient $\left(\frac{Q}{\omega D_2^2 b}\right)$
ξ = power consumption coefficient $\left(\frac{W}{\rho\omega D_2^4 b}\right)$

Superscripts and Subscripts

1 = impeller inlet
2 = impeller outlet
BEP = best efficiency point
max = maximum
s = specific
T = total

GENERAL DESCRIPTION OF THE MACHINES

All the turbomachines studied here consist of two squirrel cage fans at each side of an electrical engine. They are commonly used as part of the evaporator in air-conditioning systems for public transport (Figure 1). The fans blow the cooled air into the canalization that delivers fresh air towards the passengers inside the cabin.

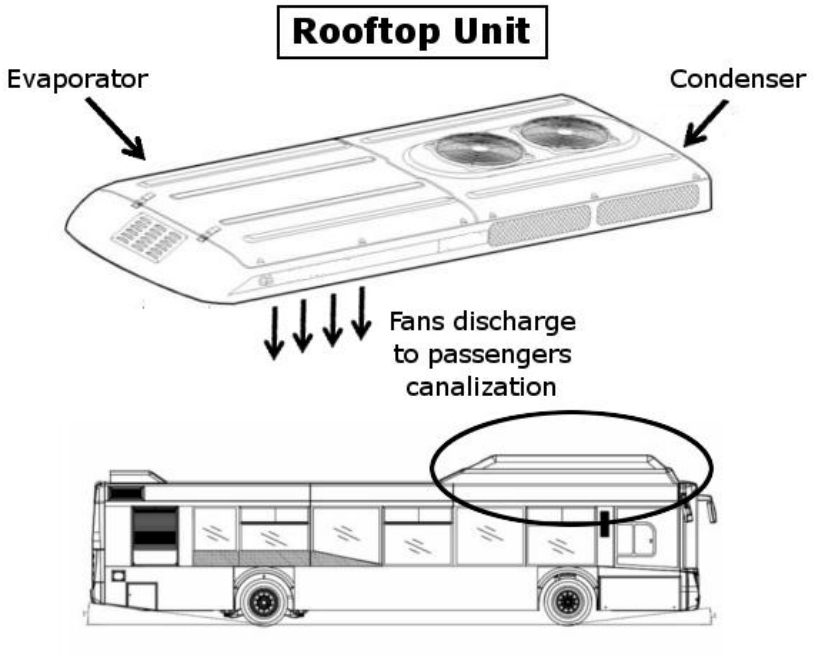

Figure 1: Rooftop unit of air-conditioning system

A generic fan configuration is shown in Figure 2. A fan casing volute comprises two impellers, which are further joined to a second module placed behind the electrical motor. Hence, each impeller has two sets of a large number of short chord forward-curved blades separated by a central plate. The discharge sections are rectangular, while the aspirations sections are circular. Due to this configuration, these machines present two differenced inlets: two free inlets, one on each side of the fan, and two partially obstructed ones on the sides close to the electrical engine. All these facts lead to the appearance of non-symmetric inlet flow conditions.

Note that the presence of the central plate is introduced to reduce the air recirculation at the inlet (Eck [3]). Moreover, it is a common practice to let the blades of each half lie half-way between those of its counterpart impeller, in order to minimize the noise component related to the tonal BPF.

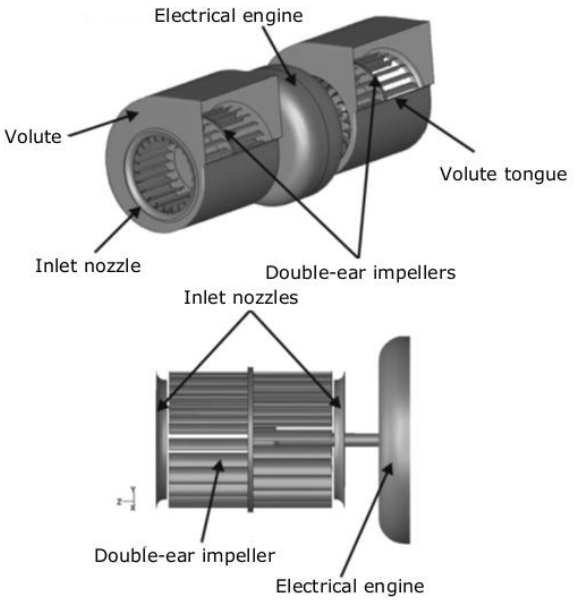

Figure 2: Generic Squirrel-Cage fan configuration

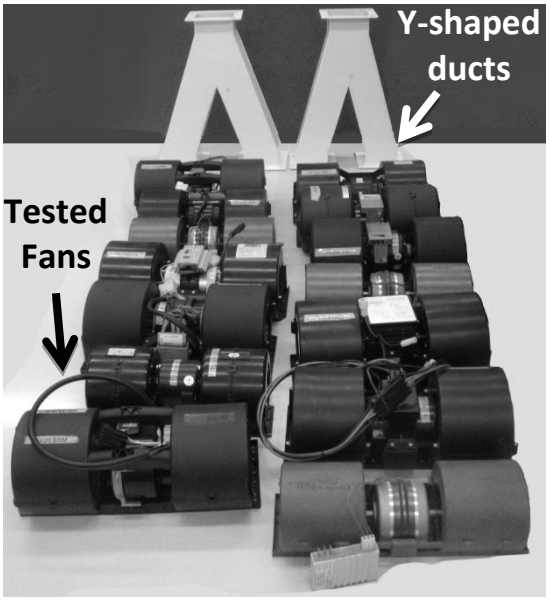

Figure 3: Tested fans and Y-shaped ducts

METHODOLOGY

First, a detailed description of geometric and construction parameters of the available equipment has been made. Figure 3 shows the different squirrel-cage fans analysed and two of the Y-shaped ducts used for the connection to the testing facility. This data collection includes diameters (impeller inlet, impeller outlet and inlet nozzle), widths (impeller and volute), thicknesses, numbers of blades, impeller-volute distances, volute inlet configurations, drive systems and building materials.

The tests for the aerodynamic and acoustic characterization of the fan have been made in a normalized ducted installation (type B according to ISO 5136 [4]). Figure 4 shows a sketch of this test installation. The flow leaving the two impellers is merged in a Y-shaped duct placed immediately downstream the outlet section. After leaving the fan, the air flows through a straightener in order to remove the swirl component generated by the fan. At the end of the facility, an anechoic termination removes undesired noise reflections and a regulation cone permits to modify the fan operating point.

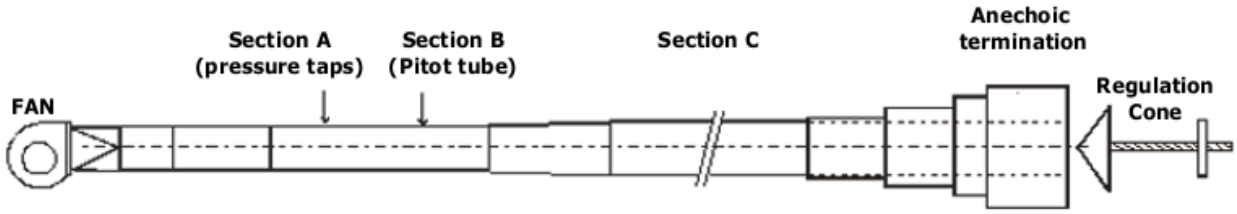

Figure 4: Sketch of the test installation

More details about the followed procedures can be found in Velarde-Suarez et al. [5]. The tests were conducted at a constant tension of 26.5 V for the electrical motor, which is a typical value during the operation of the fans in the air-conditioning system. The performance curves were obtained measuring between seven to eight points for the whole operating range of the fans, which was considered accurate to describe their overall characteristics. In each of these points, several data were collected: static pressure (Section A), dynamic pressure (Section B), electrical engine voltage and current intensity, rotation speed and acoustic pressure in the duct and in the aspirating region in the vicinity of the fan inlet. Air temperature and density in the laboratory were also recorded at the beginning of each fan characterization.

The acoustic pressure measurements have been made using two 1/2" microphones. The uncertainty of the microphones is declared by the manufacturer in 0.2 dB, with a confidence level of 95%. The signal from the microphone preamplifiers is introduced in a 2-channel real-time acquisition unit, which software is afterwards employed to postprocess the measured signals. Consequently, Lp spectrums, both inside the duct (Section C) and outside the fan (in a point located 0.5 m upstream the fan inlet), were retrieved using this procedure, typically with the microphone aligned to the impeller shaft.

RESULTS AND DISCUSSION

Morphological results

All the volutes and the impellers of the fans analysed are made of plastic materials, except for just one impeller made of aluminium (named F15 in the database). On the contrary, there is a noticeable difference between the stiffness of the plastic materials used in the construction of the impellers. In addition, nine out of fifteen impellers have 28 blades; other three have 34 blades and the last three fans have 23, 24 and 26 blades respectively.

Table 1: Maximum and minimum of various measured parameters

	ψ	Φ	n_s	d_s	D_{nozzle}/D_1	D_1/D_2	$4b/D_1$	$\Delta r/D_1$ [%]	ω [rpm]	S
Max	0.36	0.26	3.00	1.42	1.22	0.85	3.10	22.50	5170	1.58
Min	0.14	0.17	1.47	0.80	0.95	0.71	2.05	12.12	3580	0.88

Concerning other geometrical parameters, the ratio of the inlet nozzle diameter to the impeller inlet diameter, the inner-outer diameter ratio, the aspect ratio between the outlet width and the inner diameter or the impeller-tongue radial distance has been summarized for the entire database. All the dimensionless parameters are calculated for the best efficiency point. Table 1 shows the maximum and minimum values for these representative parameters in the study, as well as additional

operational information. Two tables with more detailed information can be seen in the attached Annex.

An important design parameter in this type of fans is the ratio between the diameters of the inlet nozzle and the impeller inlet (D_{nozzle}/ D_1). The presence of a "no-flow" zone over the impeller blades near the inlet can be noticed. In the region over the impeller blades near the inlet, there is little or no through flow and the blade passages contain completely separated flow (Kind and Tobin [2]). In this zone, high axial momentum dominates the inlet flow and the static pressure distribution in the hub is not enough to turn the flow in the radial direction. Due to the existence of this separated flow zone, the volute flow varies significantly with axial location. There is a first zone, near the volute inlet, where the flow has a predominant tangential component and a second area, at the midspan and central plate, where the radial component dominates the flow. In this type of fan, it is common to choose $D_{nozzle}/D_1 > 1$, in order to facilitate the incoming flow to the impeller, minimizing the flow separation zone observed in Figure 5.

As it is shown in Figure 6, the ratio between the inlet and outlet diameters of the impellers presents an almost constant value around 0.78 for most of the fans. Only a reduced number of manufacturers have chosen to design the impeller with a higher ratio (F04, F08, F12 and F15). Precisely, two models of this set (F08 and F12) are confirmed as the best designs from an aerodynamic and aeroacoustic point of view, while the others fail in other critical aspects. In particular, the F15 unit is a metallic impeller with a ratio $D_{nozzle}/D_1 < 1$ and an unusual large motor placed too close to the aspirating section. On the other hand, only two of the fans observed present a lower D_1/D_2 ratio than the previously referenced 0.78 value, which correspond to particularly small fan models (F01 and F05).

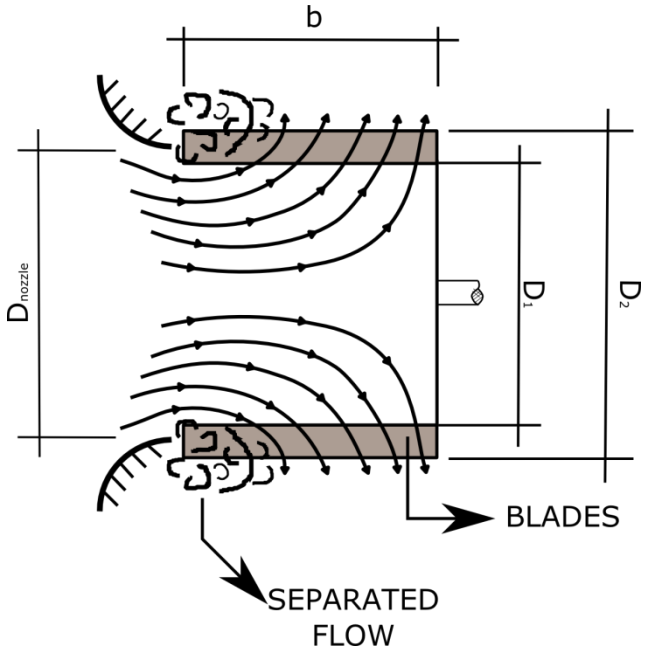

Figure 5: Separated flow in the impeller inlet

In Figure 7, the $4b/D_1$ parameter, which represents a way of measuring the flow uniformity at the inlet, is plotted. According to the literature, this parameter must be close to 1 to assure a uniform flow for this type of centrifugal fans. However, as can be noticed from the figure, the commercial fans analysed here present a width-to-diameter ratio unusually large, ranging between 2 and 3, far beyond optimum values. As a consequence, the fans present a recirculation zone at the inlet where the flow is separated and major flow disorder arises. Box A in Figure 7 points out those fans

presenting the worst ratios (F01, F04 and F05); once again, the smallest fans (named as F01 and F05) are penalized because of their reduced inlet diameters (it is important to note that the impeller width is very similar in all the cases). In the same figure, the F15 fan is the one presenting the lowest value for this ratio, though its inlet blockage ruins its flow uniformity at the inlet.

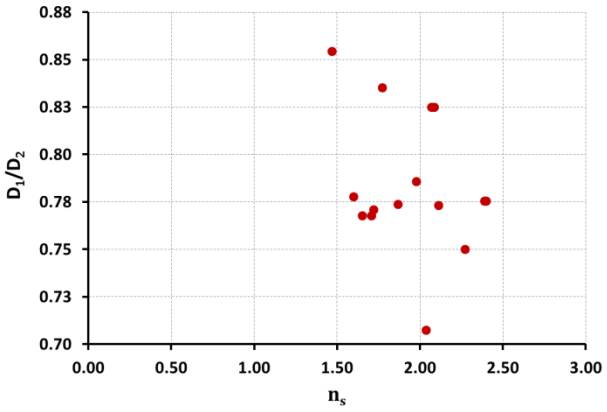

Figure 6: D_1/D_2 vs. specific speed

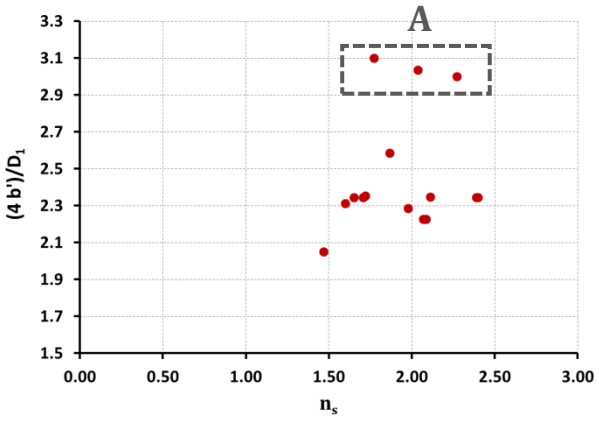

Figure 7: $4b/D_1$ vs. specific speed

A solidity parameter S has been defined as the blade chord divided by the blade spacing. Backström [6] has recommended to radial turbomachinery researchers and designers the use of solidity to correlate slip factor, that is, the rate at which centrifugal turbomachines do less work than that calculated with the assumption that the relative impeller exit flow follows the blade trailing edges. Typical values of solidity in centrifugal turbomachinery ranges from 0.5 to 2.5. In the fans analysed here, the solidity values ranges from 0.88 to 1.58, but the most frequent values are around 1.20-1.30.

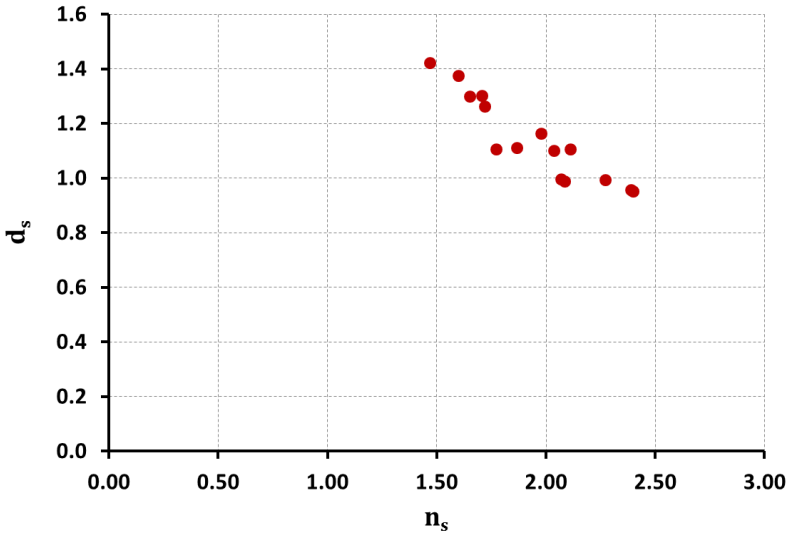

Figure 8: Specific diameter vs. specific speed

Finally, Figure 8 demonstrates that there is a linear relationship between specific speed and specific diameter. The specific speed n_s ranges from 1.5 to 2.5, while the specific diameter d_s shows values from 1 to 1.4.

Operational results

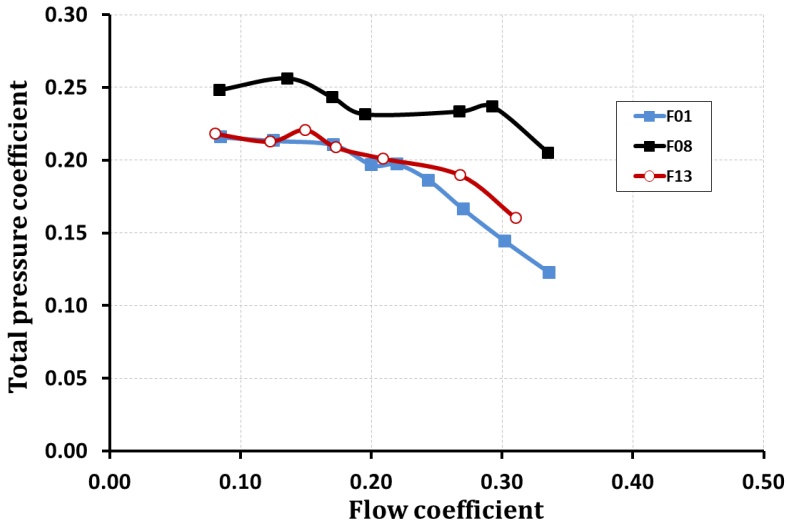

Figure 9: Performance curves for three representative fans

Performance curves for three representative fans are shown in Figure 9 as an example of the results obtained during these tests. All fans present the typical performance curves associated to forward-curved blades centrifugal fans, including instability zones. In the central flow zone, a loss of pressure followed by a recovery can be noticed in all these cases. This instability, denoted by a flat or positive slope in the performance curve, is inherent to the design of forward-curved blade fans. The authors, in previous experiences, observed an increment of unstable effects with increasing rotational speed. Thus, this unstable behaviour appears to be intensified by the poor structural stiffness of the impeller blades.

Figure 10 shows the relationship between total pressure and flow coefficients at the best efficiency point (BEP) for the different turbomachines. The total pressure coefficient and the flow coefficient are bounded between 0.18–0.27 and 0.14–0.2 respectively. Only four of the tested fans (F08, F12, F13 and F14), highlighted in the figure with the annotation (box B), reached a higher flow coefficient (around 0.27). This higher flow rate discharged is related to their large values of width-to-diameter ratio, which becomes an advantage when competing to provide an extra flow rate (this is particularly enhanced for units F08 and F12). This confirms again the strong influence of this parameter to obtain a good performance. Fans F08 and F012, with the higher pressure coefficients, have been designed with a solidity value of 1.15, in the mid range of this parameter in the present study. According to Backström [6], higher values of solidity are related to a better guiding of the flow by the blades, and thus to a real impeller work closer to the theoretical one. However, an important increment in the impeller solidity would origin at the same time increasing aerodynamic losses in the blade channels, so there is a need for a compromise in order to found an optimized value of solidity parameter: not too low in order to best guiding the flow, and not too high in order to minimize aerodynamic impeller losses. In the present study, this optimized solidity value appear to be around 1.15-1.30.

Additionally, the four best-designed fans previously mentioned are the ones presenting total efficiency values (η_t) exceeding 40%. However, the values of the total efficiency include the motor-fan consumption. Therefore, to achieve good overall performance values is important to have also a good electric motor, it is not enough to optimize the aerodynamic design of the fan.

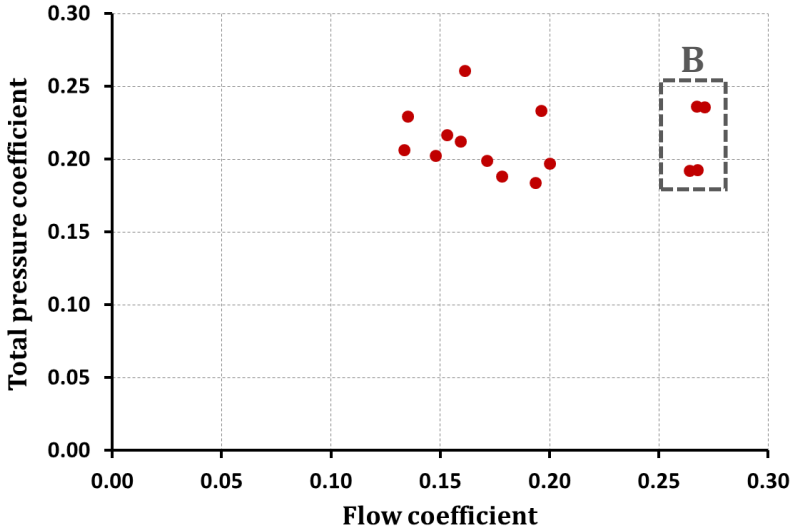

Figure 10: Total pressure coefficient vs. flow coefficient at the BEP

Acoustic results

Velarde-Suárez et al. [7] presented an aeroacoustic study on a small squirrel-cage fan for public transport. They found that the predominant tonal component in the noise generation of this fan is the blade passing frequency one. They noticed that the relevant values of the blade passing levels in these cases could be explained by the high pressure fluctuation values found, not only close to the volute tongue, but also in the rest of the volute. This fact is probably due to the size restrictions commonly suffered by these devices, which constitute a clear limitation on the volute design.

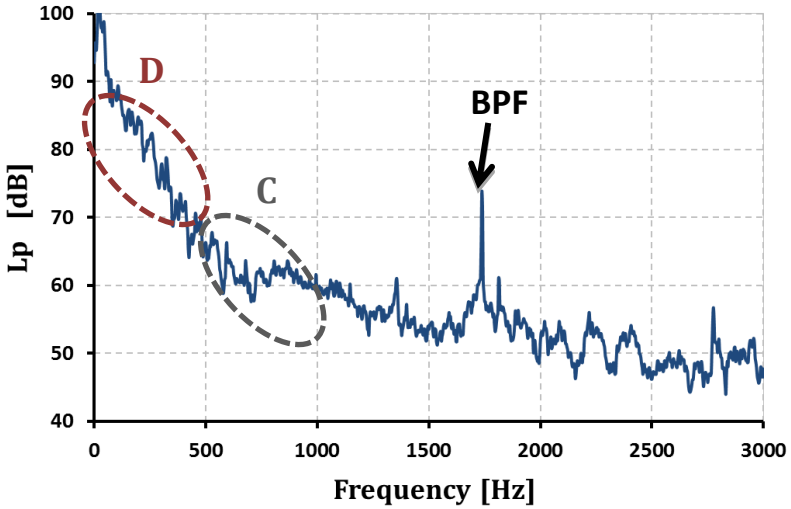

Figure 11: Lp spectrum at Qmax for the fan F01

Figure 11 represents the spectrum obtained with the microphone placed inside duct, at the maximum flow rate for the fan F01. The BPF is clearly noted as the most important tonal noise source. Another important consideration is the existence of an area of high broadband noise for mid frequencies (box C: around 500-1000 Hz). This kind of noise cannot be attributed to specific aerodynamic phenomena. However, an increment in this broadband noise has been observed when the rotating velocity increases (Velarde-Suárez et al. [5]), thus confirming the strong effect of the material stiffness in the global aeroacoustic performance. There are also high levels of noise at low

frequencies (box D: under 400 Hz). This low-frequency noise is typical of in-ducts measurements and does not appear when the measurements are made outside the test bench.

For comparing the sound pressure levels, the Lp_s parameter has been calculated as indicated in Eq.1. This parameter takes into account the operation point of the machine, the flow and the total pressure, when the noise level is measured. Figure 12 represents the total sound pressure level measured at the best efficiency point versus the distance between volute and impeller ($\Delta r/D_2$). The results do not show the expected trend, since, as pointed by Velarde-Suárez et al. [5], a reduction of the distance between volute and impeller should imply a drop in the sound levels of the fans. But looking at the figure, no relationship between the volute-impeller distance and the noise levels can be expected. This is due to the fact that the total Lp_s includes various noise sources. These sources include aerodynamic noise, mechanical noise generated by the fan and the noise produced by the electric motor.

$$Lp_s = Lp - 10\log_{10}(Q) - 20\log_{10}(P_T) \qquad (1)$$

Figure 13 shows the noise levels at the BPF for the studied machines when operating at their best efficiency point. Indeed, taking into account only the tonal component of the noise generated, there is a downwards trend in the noise levels captured when the distance between volute and impeller is increased, confirming previous results cited above.

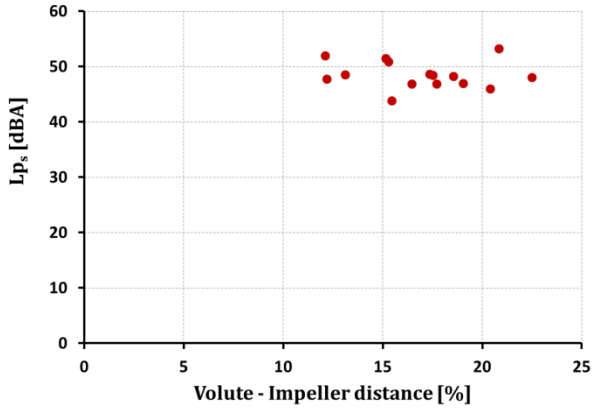

Figure 12: Lp_s vs. volute-impeller distance at the BEP

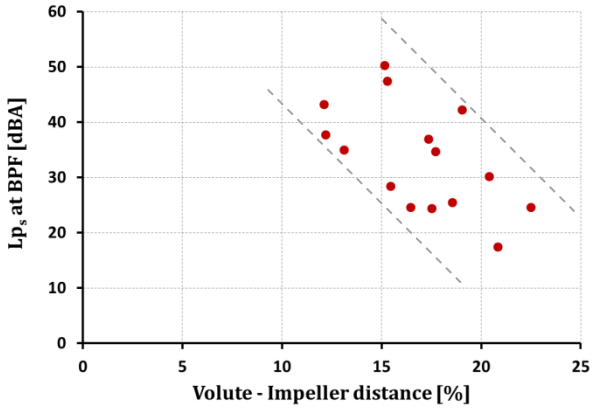

Figure 13: Lp_s vs. volute-impeller distance at the BEP

Conclusions

In this paper, a comprehensive study of the geometric characteristics, as well as an operational and acoustic characterization of several small squirrel-cage fans, used in the evaporation system for HVAC applications in public transport, was conducted. This type of turbomachines has revealed to be quite complex, and both aerodynamic and acoustic behaviour is influenced by many factors.

Different design considerations for improving performance in terms of flow parameters have been determined. The $4b/D_1$ parameter close to unity implies a greater uniformity of the flow and the relationship between the impeller diameters (D_1/D_2) must be as high as possible. The D_{nozzle}/D_1 parameter must have values above unity to avoid a blocking design of the inlet. Another design factor is the electrical motor size; an engine too big intensifies the blocking effect, with the consequent performance loss.

The acoustic results show different phenomena. One of them is the existence of high levels of broadband noise for mid-range frequencies increasing with rotating velocity. High levels of noise at low frequencies in the in-duct measurements were also noticed. Considering only the tonal aerodynamic noise, specifically the one produced at the blade passing frequency, a relationship between the noise and the volute-impeller distance can be established, resulting in lower noise levels when the volute-impeller distance is increased.

ACKNOWLEDGMENTS

The authors acknowledge the support from the "Ministerio de Ciencia e Innovación" under Project "Tecnologías ecológicas para el transporte Urbano, ecoTRANS" (CDTI).

The authors also gratefully acknowledge the collaboration and the kind permission for publication of Hispacold International S.A., with a special mention to D. Juan Bernal-Cantón, from the Department of Innovation.

BIBLIOGRAPHY

[1] Kind RJ, Tobin MG., 1990, – *Flow in a centrifugal fan of the squirrel cage type,* ASME J Turbomach, 112:84–90, **1990**

[2] Cau, G., Mandas, N., Manfrida, N. and Nurzia, F., – *Measurements of primary and secondary flows in an industrial forward-curved centrifugal fan,* ASME J. Fluids Eng., 109, pp. 353-358. **1987**

[3] Eck, B., – *Fans, Design and operation of centrifugal, axial-flow and cross-flow fans,* Pergamon Press Ltd. **1973**

[4] *International Organization for Standarization ISO 5136:1990 and Technical Corrigendum 1:1993. Determination of sound power radiated into a duct by fans. In-duct method*. **1990**

[5] Velarde-Suárez S, Ballesteros-Tajadura R., Pereiras-García, B., Santolaria-Morros, C., – *Reduction of the aerodynamic tonal noise of a forward-curved centrifugal fan by modification of the volute tongue geometry,* Applied Acoustics, Vol. 69, pp. 225–232. **2008**

[6] Backström, T.W.von., – *A Unified Correlation for Slip Factor in Centrifugal Impellers*, Journal of Turbomachinery, Vol. 128, pp. 1–10. **2006**

[7] Velarde-Suárez S, Ballesteros-Tajadura R, González, J., Pereiras-García, B., – *Relationship between volute pressure fluctuation pattern and tonal noise generation in a squirrel-cage fan,* Applied Acoustics, Vol. 70, No. 11-12. , pp. 1384-1392. **2009**

ANNEXES

Table 2: Morphological parameters

	z	**D_{nozzle}/ D_1**	**D_1/ D_2**	**$4b/D_1$**	**$\Delta r/D_1$ [%]**	**S**
F01	23	1.10	0.75	3.00	22.5	1.22
F02	26	1.09	0.77	2.58	19.1	1.21
F03	28	1.05	0.77	2.35	17.7	1.32
F04	28	1.14	0.84	3.10	16.5	0.88
F05	24	1.21	0.71	3.03	12.2	1.58
F06	28	1.03	0.77	2.35	17.5	1.31
F07	28	1.01	0.79	2.29	15.3	1.22
F08	34	1.13	0.82	2.23	15.5	1.15
F09	28	1.01	0.78	2.31	12.1	1.27
F10	28	1.00	0.77	2.34	15.2	1.35
F11	28	1.03	0.77	2.34	13.1	1.35
F12	34	1.00	0.82	2.23	18.6	1.15
F13	28	1.01	0.78	2.34	17.4	1.29
F14	28	1.22	0.78	2.34	20.4	1.29
F15	34	0.95	0.85	2.05	20.8	0.92

Table 3: Operational parameters at the BEP

	ψ	**Φ**	**η_T [%]**	**n_s**	**d_s**	**ω [rpm]**
F01	0.20	0.20	34.4	2.27	0.99	4476
F02	0.20	0.23	38.5	1.87	1.11	4244
F03	0.16	0.21	43.6	1.72	1.26	4490
F04	0.16	0.26	39.4	1.77	1.11	4141
F05	0.17	0.20	30.4	2.04	1.10	4346
F06	0.19	0.18	35.1	2.11	1.10	4646
F07	0.18	0.19	28.9	1.98	1.16	3806
F08	0.27	0.24	43.0	2.07	0.99	3940
F09	0.13	0.21	34.0	1.60	1.38	4351
F10	0.15	0.20	38.4	1.71	1.30	3930
F11	0.15	0.22	36.1	1.65	1.30	4263
F12	0.27	0.24	43.7	2.09	0.99	4384
F13	0.27	0.19	40.8	2.40	0.95	4100
F14	0.26	0.19	41.5	2.39	0.96	4220
F15	0.14	0.23	37.6	1.47	1.42	4497